

The Least-Squares Finite Element and Minimum Residual Method for Linear Hyperbolic Problems

Adin Lazuardy Firdiansyah, Nur Shofianah and Marjono
Department of Mathematics, Brawijaya University, Indonesia

Keywords: Least-Squares Finite Element Methods, Minimum Residual Method, Hyperbolic Equations.

Abstract: Many linear hyperbolic equations are applied in sciences, for example, propagation wave and transport molecules. When the boundary data is discontinuous, the solution of linear hyperbolic equation is also discontinuous. This condition influences in finding an approximate numerical method for its solution. In the paper, we focus on the least-squares finite element method to solve linear hyperbolic equation. The linear system resulting from the discretization is a symmetric and positive definite system that will be solved using minimum residual method. Some numerical experiments are tested to illustrate the validity of the method. The numerical result shows that the method can efficiently solve the continuous and discontinuous problem of linear hyperbolic equation without oscillation

1 INTRODUCTION

We consider the linear hyperbolic equations satisfying

$$\begin{aligned} \nabla \cdot (\mathbf{b}u) &= f, & \text{in } \Omega, \\ u &= g, & \text{on } \Gamma_-, \end{aligned} \quad (1)$$

where \mathbf{b} is the convection vector and Γ_- is the inflow boundary condition defined as follow

$$\Gamma_- = \{\mathbf{x} \in \partial\Omega, \mathbf{b}(\mathbf{x}) \cdot \mathbf{n}(\mathbf{x}) < 0\},$$

and $\Gamma_+ = \partial\Omega/\Gamma_-$. The linear hyperbolic equation is applied in engineering and sciences. The equation is called transport or linear advection equation.

The linear hyperbolic equation was the first introduced by Reed and Hill in 1973. The equations (1) has a discontinuous solution when the boundary data is discontinuous. We need an alternative method to signify its condition. Numerical solutions for the linear hyperbolic equation have been done with various methods, such as SUPG (Burman, 2010), Galerkin (Bochev and Choi, 2007) and least-squares finite element methods (De *et al.*, 2004). We focus our attention on solution of linear hyperbolic equation with the least-squares finite element methods.

The finite element methods have been developed by researcher for resolving the equations (1). A comparative study SUPG, Galerkin, and least-squares finite element methods had been done by Bochev and Choi in 2007. Based on numerical result for discontinuous solution, the least-squares finite element method gives a better stability (Bochev and Choi, 2007). In 2004, the linear system resulting from least-squares finite element method was solved by using algebraic multigrid methods. Algebraic multigrid methods for elliptic equations are applied to linear system from least-squares finite element methods without modifications. The result show that complexity grows slowly relative to the size of the linear system (De *et al.*, 2004). In 2004, the dual least-squares finite element method was used to solve linear hyperbolic equations. The formulation allows discontinuous in the approximate solution and then linear system resulting from dual least-squares finite element method is solved with algebraic multigrid method. Based on the numerical result, the algebraic multigrid method is success of this solver (Olson, 2004).

In the paper, we use minimum residual (MINRES) method to solve linear system resulting from least-squares finite element method. MINRES method can resolve large sparse linear system with coefficient system is a symmetric and indefinite system (Yu-Ling Lai *et al.*, 1997). This method can also be applied in symmetric and positive definite

system (Elman *et al.*, 2005). In 2017, the simple finite element method was used to solve linear hyperbolic equation. Then, numerical experiments are used to test the flexibility of the method (Mu and Ye, 2017).

We study about the least-squares finite element and minimum residual method for resolving the equations (1). The numerical simulation was conducted with several numerical experiments.

2 KNOWN RESULT

2.1 The Finite Element Space

We start by defining the standard finite element space $H^s(\Omega)$ for Sobolev space with $(\cdot, \cdot)_s$ and $\|\cdot\|_s$, where $s \geq 0$. When $s = 0$, $H^0(\Omega)$ concur with $L^2(\Omega)$. Let \mathcal{T}_h denote a partitioned domain Ω into a polygons in two dimensions. In this paper, the finite element space used is as follow

$$V_h = \{v \in L^2(\Omega) : v|_T \in P_k(T), \forall T \in \mathcal{T}_h\},$$

where $P_k(T)$ is the family of polynomials on T with rate no more than k (Mu and Ye, 2017). In this paper, we use $k = 1$.

2.2 The Minimum Residual Method

Linear system resulting from discretization is solved with minimum residual method. The linear system is a symmetric and positive definite coefficient matrix.

The minimum residual (MINRES) method is the Krylov subspace method derived from the Lanczos algorithm. The MINRES is applicable to symmetric and indefinite system as well as symmetric and positive definite system. This method adopts QR factorization to solve the tridiagonal matrix from Lanczos process. The solution can be obtained by performing QR factorization on the tridiagonal matrix employing givens rotation. The new rotation in each iteration can update QR factorization from the previous iteration. Algorithm for the minimum residual method solves the linear system $\mathbf{A}\mathbf{u} = \mathbf{F}$ (Elman *et al.*, 2005).

Algorithm 1: The Minimum Residual Method.

```

 $\mathbf{z}^{(0)} = \mathbf{0}, \mathbf{w}^{(0)} = \mathbf{0}, \mathbf{w}^{(1)} = \mathbf{0}, \mathbf{u}^{(0)} = \mathbf{0}$ 
Choose tol, compute  $\mathbf{z}^{(1)} = \mathbf{F} - \mathbf{A}\mathbf{u}^{(0)}$ 
Set  $\gamma_1 = \|\mathbf{z}^{(1)}\|$  and  $\mathbf{r} = \mathbf{z}^{(1)}$ 
Set  $\eta = \gamma_1, s_0 = s_1 = 0, c_0 = c_1 = 1$ 
for j = 1 until to converge
     $\mathbf{z}^{(j)} = \mathbf{z}^{(j-1)} / \gamma_j$ 
     $d_j = \langle \mathbf{A}\mathbf{z}^{(j)}, \mathbf{z}^{(j)} \rangle$ 
     $\mathbf{z}^{(j+1)} = \mathbf{A}\mathbf{z}^{(j)} - d_j\mathbf{z}^{(j)} - \gamma_j\mathbf{z}^{(j-1)}$  (Lanczos Process)
     $\gamma_{j+1} = \|\mathbf{z}^{(j+1)}\|$ 
     $\alpha_0 = c_j d_j - c_{j-1} s_j \gamma_j$  (Update QR factorization)
     $\alpha_1 = \sqrt{\alpha_0^2 + \gamma_{j+1}^2}$ 
     $\alpha_2 = s_j d_j + c_{j-1} c_j \gamma_j$ 
     $\alpha_3 = s_{j-1} \gamma_j$ 
     $c_{j+1} = \alpha_0 / \alpha_1, s_{j+1} = \gamma_{j+1} / \alpha_1$  (Givens rotation)
     $\mathbf{w}^{(j+1)} = (\mathbf{z}^{(j)} - \alpha_3 \mathbf{w}^{(j-1)} - \alpha_2 \mathbf{w}^{(j)}) / \alpha_1$ 
     $\mathbf{u}^{(j)} = \mathbf{u}^{(j-1)} + c_{j+1} \eta \mathbf{w}^{(j+1)}$ 
     $\eta = -s_{j+1} \eta$ 
     $\mathbf{r} = \mathbf{F} - \mathbf{A}\mathbf{u}^{(j)}$ 
    If  $\|\mathbf{r}\| \leq \text{tol}$ 
        stop
    end
end

```

where

- $\mathbf{z}^{(j)}, j = 1, 2, 3, \dots$ is the Lanczos vectors;
- c_j and $s_j, j = 1, 2, 3, \dots$ are used to compute the next rotation;
- \mathbf{r} is the residual;
- $\mathbf{u}^{(j)}, j = 1, 2, 3, \dots$ is the unknown functions;
- $\alpha_0, \alpha_1, \alpha_2, \alpha_3$ are the scalar in QR factorization.

3 RESULTS AND DISCUSSIONS

3.1 Discretization Using Least-Squares Finite Element Method

The approximate solution of (1) for $u_h \in V_h$ is

$$a(u_h, v) = l(v), \quad v \in V_h. \quad (2)$$

Since u_h belongs to V_h , it can be written as

$$u_h = \sum_{i=1}^n u_i \phi_i,$$

where ϕ_i is the basis function. The finite element method is to find the unknown u_j satisfying

$$\sum_{j=1}^n u_j \int_{\Omega} (\nabla \cdot (\mathbf{b}\phi_j)) (\nabla \cdot (\mathbf{b}\phi_i)) d\Omega = \int_{\Omega} f(\nabla \cdot (\mathbf{b}\phi_i)) d\Omega, \quad i = 1, 2, \dots, n. \quad (3)$$

3.2 Computer Implementation

Let $\{\phi_i\}_{i=1}^n$ be the basis functions for V_h with n is the number of interior nodes. Substitute $u_h = \sum_{j=1}^n u_j \phi_j$ and choose basis function $v = \phi_i, i = 1, 2, \dots, n$ in equation (2), we obtain the following linear system.

$$\sum_{j=1}^n u_j A_{i,j} = F_i, \quad i = 1, 2, \dots, n.$$

This method can be summarized in the following algorithm:

- Create a mesh triangular at domain Ω and define the space of continuous piecewise linear V with basis function $\{\phi_i\}_{i=1}^n$;
- Compute the $n \times n$ stiffness matrix A and the $n \times 1$ load vector F with entries;

$$A_{i,j} = \int_{\Omega} (\nabla \cdot (\mathbf{b}\phi_j)) (\nabla \cdot (\mathbf{b}\phi_i)) d\Omega, \quad i, j = 1, 2, \dots, n;$$

$$F_i = \int_{\Omega} f(\nabla \cdot (\mathbf{b}\phi_i)) d\Omega, \quad i = 1, 2, \dots, n;$$

- Set boundary conditions;
- Solve the linear system $\mathbf{A}\mathbf{u} = \mathbf{F}$;
- Set

$$u_h = \sum_{i=1}^n u_i \phi_i.$$

3.3 Numerical Result

In this section, we provide several numerical simulations to illustrate our method. The simulation divided into two cases, numerical simulation for cases with continuous and discontinuous solutions. The continuous solution is shown in test 1-4. The discontinuous solution is shown in test 5-9. The main goal is to verify numerically (3). We follow the algorithm in previous section. The numerical

solution is pure convection, which source terms ($f = 0$) for test 3-9. The Dirichlet boundary conditions are chosen to solve for all experiments.

The numerical simulations are solved in domain $\Omega = (0,1)^2$. The left, right, bottom, and top in domain Ω are denoted by D_L, D_R, D_B, D_T , respectively. The linear triangular element is used to define the finite element space in all simulations, see Figure 1.

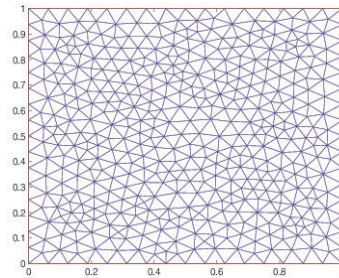


Figure 1: The linear triangular element.

The size mesh for domain Ω is estimated to use uniform grids of Ω into linear element. We estimate uniform grids with $h = 2^{-k}$ for k is positive integers between 3 until 7. All numerical experiments are similar to the tests that considered in Lin Mu and Xie Ye (2017). The numerical results are as follow.

3.3.1 Experiment 1

We use $\mathbf{b}(1,1), \Gamma_- = D_B \cup D_L$, and $u(x,y)$ for exact solution as follow:

$$u(x,y) = \sin(\pi x) \sin(\pi y).$$

The error profile is shown in Table 1.

Table 1: Error profile for experiment 1.

h	Error in experiment 1
2^{-3}	$1.6000e - 02$
2^{-4}	$3.8336e - 03$
2^{-5}	$1.0392e - 03$
2^{-6}	$2.6089e - 04$
2^{-7}	$6.9362e - 05$

It can be seen in Table 1 that the numerical result has relatively small errors.

3.3.2 Experiment 2

We borrow the same case as experiment 1, but $\mathbf{b}(1,-1)$ and $\Gamma_- = D_B \cup D_L$. The numerical result

has relatively small errors. The error profile is shown in Table 2.

Table 2: Error profile for experiment 2.

h	Error in experiment 2
2^{-3}	$1.5397e - 02$
2^{-4}	$3.6770e - 03$
2^{-5}	$1.0301e - 03$
2^{-6}	$2.6139e - 04$
2^{-7}	$7.0335e - 05$

3.3.3 Experiment 3

We use $\mathbf{b}(b_1, b_2)$ for the convection vector. We have the degree $\cos \theta$ and $\sin \theta$ with $\theta = \pi/6$ for b_1 and b_2 , respectively. $u(x, y)$ for the exact solution is as follow:

$$u(x, y) = \frac{1}{(y - \rho x - \beta)^2 + \sigma}$$

where $\rho = b_2/b_1$. We consider $\beta = 0.5$ and $\sigma = 0.1$.

The error profile is shown in Table 3. The numerical result has relatively small errors. The contour plot is shown in Figure 2.

Table 3: Error profile for experiment 3.

h	Error in experiment 3
2^{-3}	$1.6789e - 01$
2^{-4}	$4.4709e - 02$
2^{-5}	$1.5174e - 02$
2^{-6}	$3.8399e - 03$
2^{-7}	$1.0483e - 03$

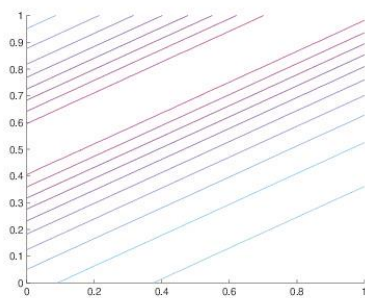


Figure 2: The contour plot for experiment 3.

3.3.4 Experiment 4

We borrow the same case as experiment 3, but $u(x, y)$ is as follow.

$$u(x, y) = \begin{cases} \frac{1}{(y - \rho x - \beta)^2 + \sigma}, & \text{if } y \geq \rho x, \\ \frac{20}{7}, & \text{if } y < \rho x. \end{cases}$$

The error profile is shown in Table 4. The numerical result has relatively small errors. The contour plot is plotted in Figure 3.

Table 4: Error profile for experiment 4.

h	Error in experiment 4
2^{-3}	$1.8099e - 01$
2^{-4}	$5.1353e - 02$
2^{-5}	$2.2329e - 02$
2^{-6}	$1.0020e - 02$
2^{-7}	$5.4454e - 03$

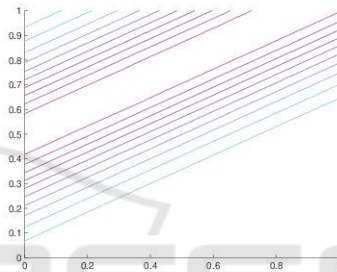


Figure 3: The contour plot for experiment 4.

3.3.5 Experiment 5

In the experiment, we use $\mathbf{b}(1, \delta), \Gamma_- = D_L \cup D_B$, and $g(x, y)$ for the boundary data is

$$g(x, y) = \begin{cases} 2, & \text{in } D_L, \\ 1, & \text{in } D_B. \end{cases}$$

The streamline function used is $y = \delta x$, where $\delta = \tan 35^\circ$.

Our experiment shows that boundary data has a profound effect upon the method. Figure 4 shows that the numerical solution is free from oscillation.

Figure 5 and 6 show the contour plot with $h = 2^{-4}$ and $h = 2^{-5}$, respectively. As can be studied, the numerical solutions on smooth mesh produce a finer approximation than numerical solutions on coarse meshes.

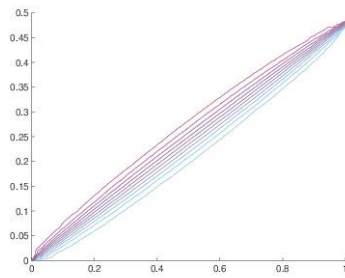


Figure 4: The contour plot for experiment 5.

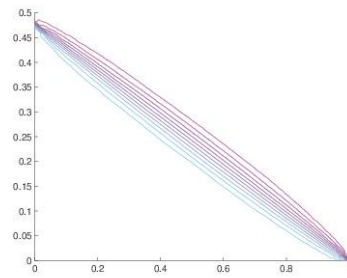


Figure 7: The contour plot for experiment 6.

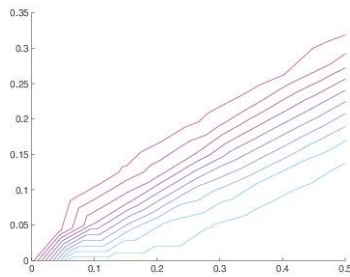


Figure 5: The contour plot for $h = 2^{-4}$.

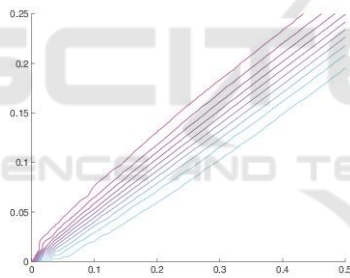


Figure 6: The contour plot for $h = 2^{-5}$.

3.3.7 Experiment 7

Here $\mathbf{b}(-y, x), \Gamma_- = D_R \cup D_B$, and $g(x, y)$ for the boundary data is

$$g(x, y) = \begin{cases} -1, & \text{in } D_B \text{ with } x < \frac{43}{64}, \\ 1, & \text{in } D_B \text{ with } x \geq \frac{43}{64}, \\ 1, & \text{in } D_R. \end{cases}$$

The contour plot is plotted in Figure 8. Figure 8 shows that the solution is free from oscillation.

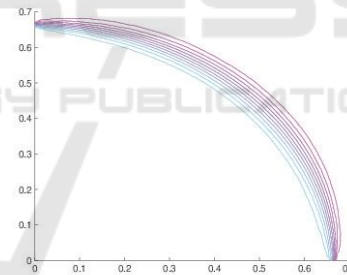


Figure 8: The contour plot for experiment 7.

3.3.6 Experiment 6

This experiment is the same as experiment 5, but $\mathbf{b}(-1, \delta), \Gamma_- = D_R \cup D_B$, and $g(x, y)$ is given as follow.

$$g(x, y) = \begin{cases} 2, & \text{in } D_R, \\ 1, & \text{in } D_B. \end{cases}$$

The streamline function used is $y = -\delta x$. The contour plot is plotted in Figure 7. Again, our solution is free from oscillation.

3.3.8 Experiment 8

In this experiment, we use $\mathbf{b}(y, 1 - x), \Gamma_- = D_L \cup D_B$, and $g(x, y)$ chosen is as follow.

$$g(x, y) = \begin{cases} 1, & \text{in } D_B \text{ with } x < \frac{21}{64}, \\ -1, & \text{in } D_B \text{ with } x \geq \frac{21}{64}, \\ 1, & \text{in } D_L. \end{cases}$$

The numerical solution for experiment 8 that shown in Figure 9 shows that the solution is also free from oscillation.

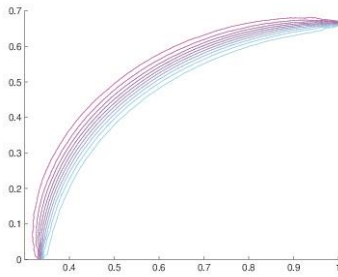


Figure 9: The contour plot for experiment 8.

3.3.9 Experiment 9

In the last experiment, we use $\mathbf{b}(y, 0.5 - x)$ and

$$g(x, y) = \begin{cases} 0, & \text{if } x = 0, 0 \leq y \leq 1, \\ 0, & \text{if } y = 1, 0.5 \leq x \leq 1, \\ 0, & \text{if } y = 0, 0 \leq x \leq 0.17, \\ 1, & \text{if } y = 0, 0.17 \leq x \leq 0.33, \\ 0, & \text{if } y = 0, 0.33 \leq x < 0.5. \end{cases}$$

The contour plot for experiment 9 is plotted in Figure 10. The conclusion obtained is the same conclusion as the previous experiment.

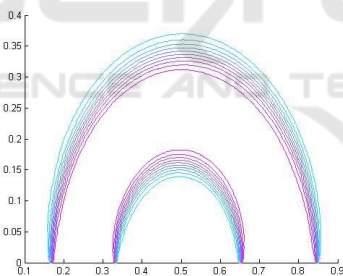


Figure 10: The contour plot for experiment 9.

4 CONCLUSIONS

Based on the previous section, it can be concluded that the least-squares finite element and minimum residual method can efficiently solve the linear hyperbolic equation without oscillation. The numerical result shows that the numerical error is relatively small for continuous problem. In addition, the solution is free from oscillation for discontinuous problem.

REFERENCES

- Bochev, P. B., Choi, J., 2007. A Comparative Study of Least-squares, SUPG and Galerkin Methods for Convection Problems. *International Journal of Computational Fluid Dynamics* Vol. 15. pp. 127-146, Overseas Publishers Association.
- Burman, E., 2010. Consistent SUPG-Method for Transient Transport Problems: Stability and Convergence. *Computer Methods in Applied Mechanics and Engineering* Vol.119, pp. 1114-1123. Elsevier.
- De, H. S., Manteuffel, T. A., McCormick, S.F., 2004. Least-Squares Finite Element Methods and Algebraic. *SIAM J. SCI. COMPUT* Vol. 26. No. 1. pp. 31-54. Society for Industrial and Applied Mathematics.
- Elman, H., Silvester, D., Wathen, A., 2005. *Finite Elements and Fast Iterative Solvers: with Application in Incompressible Fluid Dynamics*, Oxford University Press, New York.
- Mu, L., Ye, X., 2017. A Simple Finite Element Method for Linear Hyperbolic Problems. *Journal of Computational and Applied Mathematics* Vol.330, pp. 330-339. Elsevier.
- Olson, L., 2004. A Dual Least-Squares Finite Element Method for Linear Hyperbolic PDEs: A Numerical Study. *Department of Applied Mathematics*.
- Reed, W. H., Hill, T. R., 1973. Triangular Mesh Methods for the Neutron Transport Equation. *Technical Report LA-UR-73-479*. Los Alamos Scientific Laboratory.
- Yu-Ling Lai, Wen-Wei Lin, Pierce, D., 1997. Conjugate gradient and minimal residual methods for solving symmetric indefinite systems. *Journal of Computational and Applied Mathematics* Vol. 84. pp. 243-256, Elsevier.